Multipath-Aware Hybrid Beamforming in Upper Mid-Band via Lightweight Neural Network

Hyeongjun Kim, Hyung Joon Cho, and Byonghyo Shim

Institute of New Media and Communications Department of Electrical and Computer Engineering
Department of Electrical and Computer Engineering, Seoul National University
Seoul, Korea

Email: {hjkim, hjcho}@islab.snu.ac.kr, bshim@snu.ac.kr

Abstract—The upper mid-band (FR3, 7.125 - 24.25 GHz) of 6G presents unique challenges for beamforming due to its lower path loss and richer multipath effects compared to the mmWave (FR2, 24.25 - 52.6 GHz). Traditional narrow, highly directional beamforming designed for FR2 can lead to suboptimal performance in FR3, as it neglects the richer set of usable propagation paths present in this band. In this work, we propose a practical hybrid beamforming design for FR3 that explicitly exploits these multipath characteristics, with a simple, lightweight deep neural network employed to assist in estimating pathwise weights. The design adaptively prioritizes and combines multipath components to improve overall transmission quality. Experimental results show that this approach enables more reliable and robust beamforming performance with modest model complexity, highlighting its potential for practical deployment in next generation mobile systems.

I. INTRODUCTION

In the evolution toward 6G wireless systems, the upper midband (FR3, 7.125 - 24.25 GHz) has emerged as a critical frequency range, offering a balance between coverage and capacity for dense urban deployments. Beamforming in FR3 faces unique challenges compared to both sub-6GHz (FR1) and mmWave (FR2) frequencies. While FR2 is characterized by highly directional and sparse propagation, FR3 channels exhibit moderate path loss alongside richer multipath propagation [1]–[4]. In this regime, conventional narrow or single-path beamforming techniques, which maximize signal power around the strongest path, fail to capitalize on the additional spatial diversity available in the channel. To address this limitation, multipath-aware beamforming aims coherently combine distinct propagation paths, reinforcing the received signal and improving robustness against blockage and fading.

Traditional analog beamforming architectures, commonly adopted for implementing narrow beams, are fundamentally limited for multipath exploitation: they can only manipulate the phase of transmitted signals. To generate multiple beams the analog arrays must be divided into sub-arrays. However, this division reduces the array gain per beam and restricts the flexibility of the beam pattern [5]. Meanwhile, fully digital beamforming, which enables independent phase and amplitude control at each antenna, allows for the optimal combining of all significant multipath components. As a result, digital beamforming achieves far superior performance, but it remains

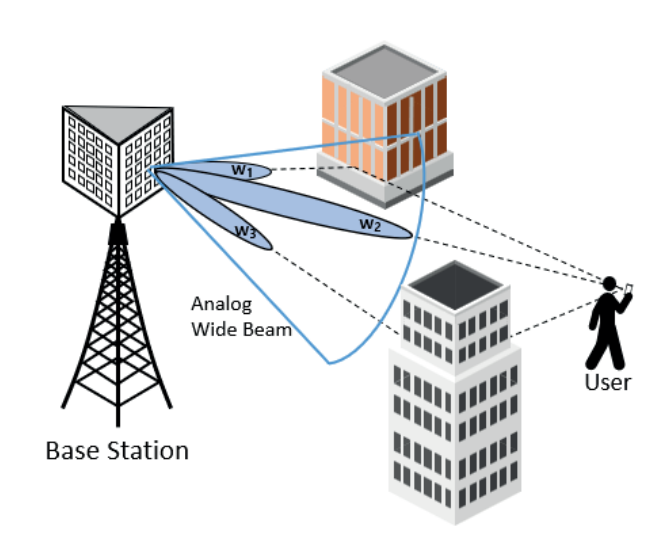


Fig. 1. Concept of downlink multipath-aware hybrid beamforming.

prohibitively expensive and power-consuming for practical systems.

Hybrid beamforming is a widely studied compromise to overcome the limitations of analog and fully digital beamforming [6], [7]. In hybrid architectures, a limited number of digital RF chains are used together with analog phase shifters to control a large antenna array. This architecture enables flexible beam steering while keeping hardware cost and power consumption manageable, making hybrid beamforming an effective solution for FR3.

Within the hybrid MIMO architecture, we propose a practical multipath-aware beamforming scheme tailored for FR3 channels. In our approach, the codebook based analog beamformer implements wide beams, that span sufficiently broad angular sectors to encompass multiple significant propagation paths simultaneously. Inspired by the Type-II codebooks in 3GPP NR [8], the digital baseband precoder is computed by a weighted sum of the effective steering vectors associated with each usable path within the wide beam's coverage. The weights are derived via a lightweight neural network that maps the geometric channel parameters (e.g., angle, gain, delay) to complex coefficients optimized for the received signal

strength. We adopt a lightweight network to leverage deep learning's capability to model complex nonlinear mappings, while keeping the model simple enough for real-time deployment. Our method enables robust and efficient beamforming for FR3, while maintaining the practical feasibility and low complexity. This concept is illustrated in Fig. 1, which depicts how multiple significant paths can be used to reinforce signal transmission within a hybrid beamforming framework.

II. FR3 HYBRID MIMO SYSTEM

A. Hybrid Beamforming

We consider a single stream downlink transmission scenario where the base station (BS) is equipped with $N_t = N_x \times N_y$ uniform planar antenna (UPA) elements and employs hybrid beamforming with $N_{\rm rf}$ RF chains to serve a single antenna user. The received signal y at the user is given by

$$y = \mathbf{h}^{\mathrm{H}} \mathbf{F}_{\mathrm{RF}} \mathbf{f}_{\mathrm{BB}} s + n, \tag{1}$$

where $\mathbf{h} \in \mathbb{C}^{N_t \times 1}$ denotes the downlink channel vector from the BS to the UE and $n \sim \mathcal{CN}(0, \sigma_n^2)$ is the additive Gaussian noise. $\mathbf{F}_{\mathrm{RF}} \in \mathbb{C}^{N_t \times N_{\mathrm{rf}}}$ is the analog RF beamformer, and $\mathbf{f}_{\mathrm{BB}} \in \mathbb{C}^{N_{\mathrm{rf}} \times 1}$ is the digital baseband precoder. The overall beamformer is subject to the power constraint $||\mathbf{F}_{\mathrm{RF}}\mathbf{f}_{\mathrm{BB}}||^2 \leq P_{\mathrm{t}}$, where P_{t} is the transmit power budget.

The analog beam is realized using phase shifters, so every nonzero element of $|[\mathbf{F}_{\mathrm{RF}}]_{i,j}|$ has constant unit modulus. To ensure practical feasibility, \mathbf{F}_{RF} is not adaptively optimized for each instantaneous channel realization but is instead selected from a finite codebook of candidate beams. These beams are implemented as wide beams designed to span sufficiently broad angular sectors, thereby encompassing multiple significant multipath components simultaneously. In this work, we construct the codebook using the DFT matrix, which enables the analog beamformer to generate directional beams with low hardware complexity.

In our scenario, we adopt a partially connected hybrid architecture described in [7] and demonstrated in Fig. 2. This configuration achieves lower hardware complexity and power consumption compared to its fully connected counterpart. Each RF chain is connected to a dedicated subarray with $n_t = n_x \times n_y = N_t/N_{\rm rf}$ antenna elements in this configuration. The analog beamforming matrix is given by

$$\mathbf{F}_{\mathrm{RF}} = \mathrm{diag}\left(\begin{bmatrix} \mathbf{f}_{\mathrm{RF},1} & \cdots & \mathbf{f}_{\mathrm{RF},\mathrm{N}_{\mathrm{rf}}} \end{bmatrix}\right), \quad \mathbf{f}_{\mathrm{RF}} \in \mathbb{C}^{n_t \times 1}, \quad (2)$$

where \mathbf{F}_{RF} is block-diagonal, and each block $\mathbf{f}_{\mathrm{RF},i}$ corresponds to the analog beamforming vector applied to the *i*th subarray. In the typical case, all N_{rf} blocks are chosen to be identical to implement the wide beams.

The combined effect of the physical channel \mathbf{h} and the analog beamformer \mathbf{F}_{RF} is represented by the effective channel $\mathbf{g} = \mathbf{F}_{\mathrm{RF}}^{\mathrm{H}} \mathbf{h} \in \mathbb{C}^{N_{\mathrm{rf}}}$, such that the signal model in (1) becomes

$$y = \mathbf{g}^{\mathrm{H}} \mathbf{f}_{\mathrm{BB}} s + n. \tag{3}$$

Based on this model, the achievable rate is given by

$$R = \log_2 \left(1 + \frac{P_{\rm t} |\mathbf{g}^H \mathbf{f}_{\rm BB}|^2}{\sigma_n^2} \right),\tag{4}$$

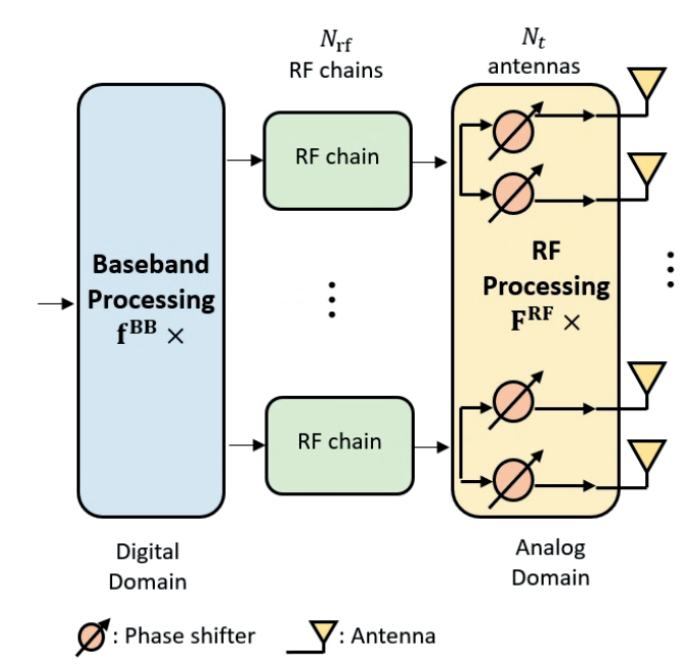


Fig. 2. Partially connected hybrid beamforming architecture.

where $|\mathbf{g}^H \mathbf{f}_{BB}|$ denotes the beamforming gain.

B. Channel Model

As for the channel model, we consider the geometric model where the channel is expressed as

$$\mathbf{h} = \sum_{l=1}^{L} \alpha_l e^{-j2\pi f_c \tau_l} \mathbf{a}(\theta_l, \phi_l) \in \mathbb{C}^{N_t \times 1}, \tag{5}$$

where L is the number of propagation paths, f_c is the carrier frequency, α_l is the complex path gain of the lth path, τ_l is the corresponding delay, θ_l and ϕ_l are the azimuth and elevation angles, respectively. The array response vector $\mathbf{a}(\theta,\phi) \in \mathbb{C}^{N_t \times 1}$ of the UPA is given by

$$\mathbf{a}(\theta, \phi) = \frac{1}{\sqrt{N_t}} \begin{bmatrix} 1 & \cdots & e^{j\pi(N_x - 1)\cos\theta\sin\phi} \end{bmatrix}^{\mathrm{T}}$$

$$\otimes \begin{bmatrix} 1 & \cdots & e^{j\pi(N_y - 1)\cos\phi} \end{bmatrix}^{\mathrm{T}}.$$
(6)

Thus, the lth path is fully characterized by the set of parameters $\{\theta_l,\phi_l,\alpha_l,\tau_l\}$. The overall channel between the BS and the user can therefore be compactly represented by the parameter vectors $\boldsymbol{\theta} = \begin{bmatrix} \theta_1 & \theta_2 & \cdots & \theta_L \end{bmatrix}, \boldsymbol{\phi} = \begin{bmatrix} \phi_1 & \phi_2 & \cdots & \phi_L \end{bmatrix}, \boldsymbol{\alpha} = \begin{bmatrix} \alpha_1 & \alpha_2 & \cdots & \alpha_L \end{bmatrix}, \boldsymbol{\tau} = \begin{bmatrix} \tau_1 & \tau_2 & \cdots & \tau_L \end{bmatrix}.$

III. MULTIPATH-AWARE BEAMFORMING DESIGN VIA LEIGHTWEIGHT NETWORK

In this work, we assume that the channel parameters of all significant paths—namely the angles of departure, complex gains, and delays—are perfectly known at the transmitter. In practice, such information can be obtained through estimation techniques including subspace-based methods [9], compressed

sensing [10], [11], or deep learning based approaches [12], [13]. Although this assumption may be optimistic, it allows us to focus on the core problem at hand: determining the optimal multipath-aware beamforming design under practical hybrid constraints. By considering the ideal case of perfect channel knowledge, we analyze the performance limits and design principles for learning the relations between the paths, without the confounding effects of estimation errors. This provides theoretical insight and serves as a reference for future research considering more realistic channel acquisition.

A. Analog Beam Selection

The objective is to identify the optimal analog beamformer $\mathbf{F}_{\mathrm{RF}}^{(k)}$, and design the digital precoder \mathbf{f}_{BB} for multipath aware beamforming. As discussed in Section II-A, \mathbf{F}_{RF} is not adaptively optimized for each channel realization, but is instead selected from a predetermined codebook of candidate analog beams. At this stage, the goal is to choose $\mathbf{F}_{\mathrm{RF}}^{(k)}$ so as to maximize the effective channel gain $||\mathbf{g}|| = ||\mathbf{F}_{\mathrm{RF}}^{\mathrm{H}}\mathbf{h}||$. This selection can be formulated as the following optimization problem.

$$\begin{aligned} & \max_{k} & || (\mathbf{F}_{RF}^{(k)})^{H} \mathbf{h} || \\ & \text{s.t.} & \mathbf{F}_{RF}^{(k)} \in \mathcal{F}_{RF} = \{ \mathbf{F}_{RF}^{(1)}, \cdots, \mathbf{F}_{RF}^{(K)} \}, \end{aligned} \tag{7}$$

where \mathcal{F}_{RF} denotes the set of analog beams, i.e., the analog beam codebook. Since the cardinality of \mathcal{F}_{RF} is limited, the above optimization can be efficiently solved via exhaustive search (beam sweeping) over all codebook entries.

B. Path Filtering

After selecting the best $\mathbf{F}_{\mathrm{RF}}^{(k)}$ for transmission, we filter the multipath components to retain only those whose directions are within the coverage of the selected analog beam. Specifically, we consider the half-power beamwidth (HPBW) [14], which for a UPA with antenna spacings of $d_x = d_y = \lambda/2$, is approximately

$$HPBW_{azimuth} \approx \frac{101^{\circ}}{n_x}$$
 $HPBW_{elevation} \approx \frac{101^{\circ}}{n_y}.$ (8)

Any path with azimuth and elevation angles (θ_l, ϕ_l) outside the HPBW region $\mathcal{A}^{(k)}$ of the selected analog beam is regarded as unusable and discarded. Consequently, only the channel paths effectively covered by $\mathbf{F}_{\mathrm{RF}}^{(k)}$ are retained for hybrid beamforming. We denote the parameters of these usable paths as $\{\tilde{\boldsymbol{\theta}}, \tilde{\boldsymbol{\phi}}, \tilde{\boldsymbol{\alpha}}, \tilde{\boldsymbol{\tau}}\}$, where only the parameters such that $(\theta_l, \phi_l) \in \mathcal{A}^{(k)}$ are included. After the filtering process, only a \tilde{L} paths remain, with $\tilde{\boldsymbol{\theta}}, \tilde{\boldsymbol{\phi}}, \tilde{\boldsymbol{\alpha}}, \tilde{\boldsymbol{\tau}} \in \mathbb{C}^{\tilde{L}}$.

C. Digital Precoding Design Principle

To enable effective multipath-aware beamforming, we next design the digital precoding vector \mathbf{f}_{BB} . Motivated by the Type-II codebook framework, we adopt a dictionary-based approach in which each resolvable path is represented by a

distinct steering vector. Accordingly, we construct a matrix of array steering vectors corresponding to the directions of the \tilde{P} usable paths:

$$\mathbf{A} = \begin{bmatrix} \mathbf{a}(\tilde{\theta}_1, \tilde{\phi}_1) & \cdots & \mathbf{a}(\tilde{\theta}_{\tilde{L}}, \tilde{\phi}_{\tilde{L}}) \end{bmatrix} \in \mathbb{C}^{N_t \times \tilde{L}}.$$
 (9)

Since the analog beamforming stage imposes a structural constraint on the realizable beams, we apply the pseudo-inverse of the analog beamformer to mitigate this distortion. This yields the effective dictionary matrix:

$$\mathbf{B} = \mathbf{F}_{\mathrm{RF}}^{\dagger} \mathbf{A} \in \mathbb{C}^{N_{\mathrm{rf}} \times \tilde{L}}.$$
 (10)

The purpose of this transformation is to ensure that the resulting hybrid beam, i.e., $\mathbf{F}_{\mathrm{RF}}\mathbf{f}_{\mathrm{BB}}$, approximates the desired multipath beam pattern given by a weighted combination of steering vectors: $\sum_{l=1}^{\tilde{L}} w_l \mathbf{a}(\tilde{\theta}_l, \tilde{\phi}_l) = \mathbf{A}\mathbf{w}$. Here the complex weights w_l jointly capture both phase and amplitude. Accordingly, the digital precoder is derived as:

$$\hat{\mathbf{f}}_{\mathrm{BB}} = \beta \mathbf{B} \mathbf{w} \tag{11}$$

where $\mathbf{w} = \left[w_1 \cdots w_{\tilde{L}}\right] \in \mathbb{C}^{\tilde{L}}$ contains the path-specific complex weights, and $\beta = \sqrt{\frac{P_t}{||\mathbf{F}_{\mathrm{RF}}\mathbf{B}\mathbf{w}||^2}} \in \mathbb{R}$ is the scaling factor that enforces the power constraint.

D. Lightweight Network for Weight Estimation

We employ a lightweight deep learning network to learn the nonlinear mapping from the filtered channel parameters $\{\tilde{\theta}, \tilde{\phi}, \tilde{\alpha}, \tilde{\tau}\}$ to the beamforming weight vector \mathbf{w} .

$$f(\tilde{\boldsymbol{\theta}}, \tilde{\boldsymbol{\phi}}, \tilde{\boldsymbol{\alpha}}, \tilde{\boldsymbol{\tau}}; \eta) = \mathbf{w},$$
 (12)

where η denotes the model parameters.

To implement this mapping, we adopt a simple feedforward neural network consisting of multiple fully connected (FC) layers with ReLU activation is employed. The mapping is structured as a composition of linear and nonlinear operations:

$$f(\mathbf{x}) = \mathbf{W}_n \sigma(\cdots(\sigma(\mathbf{W}_1(\mathbf{x}) + \mathbf{b}_1))) + \mathbf{b}_n \qquad (13)$$

where \mathbf{x} is the input feature vector, $\sigma(\cdot)$ the ReLU, and $\mathbf{W}_i, \mathbf{b}_i$ represents the weights and biases of the *i*th fully connected affine transformation. While more sophisticated architectures could potentially be considered, our aim is to demonstrate that accurate path-wise weight estimation and near-optimal beamforming performance can be achieved even with a compact neural network. This choice further aligns with practical deployment scenarios where low latency, energy-efficient inference at the BS is essential. Empirical results in Section IV-B show that the lightweight FCN effectively captures the underlying mapping of (12).

To train the model, we leverage a loss function based on the beamforming gain for the effective channel $\mathbf{g} = \mathbf{F}_{RF}^H \mathbf{h}$, explicitly incorporating the transmit power constraint. The loss is defined as:

$$\mathcal{L} = -\frac{|\mathbf{g}^{H}\hat{\mathbf{f}}_{BB}|}{|\mathbf{g}^{H}\mathbf{f}_{BB,opt}|} = -\frac{\beta|\mathbf{g}^{H}\mathbf{B}\mathbf{w}|}{\sqrt{P_{t}}||\mathbf{g}||},$$
 (14)

where $\mathbf{g}^H \mathbf{B} \mathbf{w}$ represents the projection of the hybrid beam onto the effective channel. The normalization by $\sqrt{P_t}||\mathbf{g}||$ ensures the metric is invariant to channel norm and transmit power. This loss function guides the neural network to infer a weight vector \mathbf{w} that maximizes the effective received signal strength at the user, while remaining consistent with the hardware constraints imposed by hybrid beamforming.

Notably, the denominator incorporates the optimal beamforming gain, corresponding to the maximum ratio transmission (MRT) solution for the effective channel, i.e.,

$$\mathbf{f}_{\mathrm{BB,opt}} = \sqrt{P_{\mathrm{t}}} \frac{\mathbf{g}}{||\mathbf{g}||}.$$
 (15)

Normalizing the beamforming gain by this optimal value $|\mathbf{g}^H \mathbf{f}_{\mathrm{BB,opt}}|$, ensures that it is bounded for stable training, and enables direct interpretation of the loss as the relative performance gap with respect to the optimal beamformer.

By minimizing this loss, the network learns to produce a digital precoder that approaches maximum achievable gain to the user over the selected analog beam and the channel. Hybrid beamforming performance is optimized while accounting for both hardware constraints and the inherent multipath characteristics of FR3 channels.

IV. SIMULATIONS AND DISCUSSIONS

A. Simulation Setup

In our simulations, the dataset is generated from ray tracing on OpenStreetMap models of real urban environments. Users are randomly placed within a 200 m radius of the BS, consistent with the urban microcell (UMi) deployment scenario specified in 3GPP TR 38.901 [15]. The BS is positioned at a height of 1.5 m, in accordance with UMi specifications. For each user location, ray tracing is used to extract the multipath channel parameters, as illustrated in Fig. 3. Both LOS and NLOS cases are generated, and analog beam selection and path filtering is performed prior to model training.

The BS is equipped with a UPA of $N_t=256~(16~{\rm by}~16)$ antennas and $N_{\rm rf}=64~{\rm RF}$ chains, with each RF chain connected to a $n_t=4~(2~{\rm by}~2)$ subarray. Under this configuration, the analog beam exhibits HPBW of approximately 25.5° in both azimuth and elevation, as given by (8). The carrier frequency is set to 7.5 GHz.

To ensure diversity and generalization, we construct a dataset of 10,000 samples spanning 5 different city maps. The neural network consists of 3 FC layers (n=3): the first hidden layer has 64 units, the second contains 32 units, and ReLU activation is applied after each hidden layer. Early stopping with a patience of 5 epochs is employed to prevent overfitting.

B. Evaluation and Discussions

To evaluate the effectiveness of the proposed path-wise beamforming method, we compare it against two baseline hybrid beamforming schemes.

• Single-path (Strongest-path) Beamforming: In this baseline, the analog and digital beamformers are designed to maximize the gain along the single strongest path (i.e.,



Fig. 3. Ray tracing in urban environment via OpenStreetMap file for data generation.

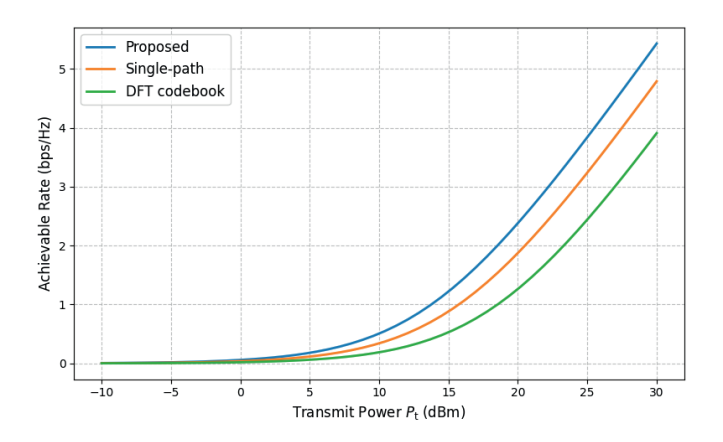


Fig. 4. Achievable Rate vs. Transmit Power $P_{\rm t}$ for different beamforming schemes in 256×64 FR3 hybrid MIMO system.

the path with the largest path gain). This approach serves as a reference case where multipath components are not exploited.

DFT Codebook-based Beamforming: In this scheme, both the analog beamformer and the digital precoder are designed based on DFT-based codebooks. Similar to the analog beam, the digital precoder f_{BB} is constrained to be one of the codebook vectors and is selected via beam sweeping. This design follows the principle of the NR Type 2 codebook [8], which employs DFT-based structures for both analog and digital domains to enable practical implementation.

For a fair comparison, all methods are implemented under the same partially connected hybrid beamforming architecture, with identical analog beam codebooks and hardware constraints as the proposed scheme. Performance is evaluated on unseen ray-traced channel datasets and using system parameters described in Section IV-A.

Fig. 4 illustrates the achievable rate as a function of the

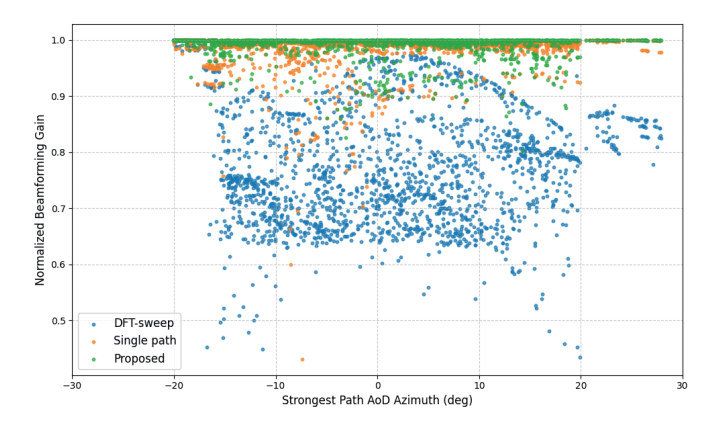


Fig. 5. Distribution of Normalized Beamforming Gain for 2,000 users vs. azimuth of each users' strongest path. The x axis is based on the strongest path direction (not necessarily LOS) to reflect both LOS and NLOS scenarios.

transmit power $P_{\rm t}$ for the proposed path-wise beamforming scheme, the single-path (strongest-path) baseline, and the DFT codebook-based baseline. The proposed scheme consistently outperforms both baselines across the entire $P_{\rm t}$ range. The rate gap becomes more evident with increasing transmit power. At a representative transmit power of $P_{\rm t}=20$ dBm, the proposed scheme achieves an average rate of 2.382 bps/Hz, which corresponds to a 27.1% improvement over the singlepath baseline (1.875 bps/Hz) and an 88.5% improvement over the DFT codebook baseline (1.264 bps/Hz). This performance gain arises from the ability of the proposed model to exploit multiple multipath components by optimally combining their amplitudes and phases. In contrast, the single-path method relies solely on the strongest path, while the DFT codebook approach is further limited by its restricted set of beam directions in both analog and digital domains.

Fig. 5 shows a scatter plot of the normalized beamforming gain

$$\frac{|\mathbf{g}^{\mathrm{H}}\mathbf{f}_{\mathrm{BB}}|}{||\mathbf{g}|| \cdot ||\mathbf{f}_{\mathrm{BB}}||} \tag{16}$$

for 2,000 randomly located users under the three considered schemes. The absence of users outside the angular range of -20° to $+20^{\circ}$ results from the directional constraint imposed by the analog beam. The proposed method (green) achieves near-optimal normalized gain for the vast majority of users across the azimuth range, with most points tightly clustered around 1. The single-path baseline (orange) also attains high gains for many users but exhibits greater variability, particularly in NLOS scenarios or when significant multipath components are present. The DFT codebook-based method (blue) displays a much wider spread and lower average gain, especially for users whose dominant path angles do not align with the quantized codebook directions. Overall, the scatter plot highlights the robustness of the proposed scheme to variations in user position and channel conditions.

V. CONCLUSION

In this paper, we proposed a novel multipath-aware beamforming approach for practical hybrid MIMO systems in FR3 band. The method leverages a lightweight deep learning model to directly learn the optimal weights for combining significant multipath components. Simulation results based on realistic urban microcell scenarios and ray-traced channel data demonstrate that the proposed scheme outperforms the baselines across a range of transmit powers and diverse user conditions. Future work will address the impact of imperfect channel parameter estimation, extend the approach to multiuser scenarios, and explore online learning techniques for real-time adaptation.

REFERENCES

- S. Kang et al., "Cellular Wireless Networks in the Upper Mid-Band," IEEE Open Journal of the Communications Society," vol. 5, pp. 2058–2072, Apr. 2024.
- [2] D. Shakya et al., "Comprehensive FR1(C) and FR3 Lower and Upper Mid-Band Propagation and Material Penetration Loss Measurements and Channel Models in Indoor Environment for 5G and 6G," in IEEE Open Journal of the Communications Society, vol. 5, pp. 5192-5218, 2024.
- [3] H. Lee et al., "Towards 6G hyper-connectivity: Vision, challenges, and key enabling technologies," in Journal of Communications and Networks, vol. 25, no. 3, pp. 344-354, June 2023
- [4] Y. Ahn et al., "Toward Intelligent Millimeter and Terahertz Communication for 6G: Computer Vision-Aided Beamforming," in IEEE Wireless Communications, vol. 30, no. 5, pp. 179-186, October 2023
- [5] I. Aykin, B. Akgun and M. Krunz, "Multi-beam Transmissions for Blockage Resilience and Reliability in Millimeter-Wave Systems," in IEEE Journal on Selected Areas in Communications, vol. 37, no. 12, pp. 2772-2785, Dec. 2019.
- [6] A. F. Molisch et al., "Hybrid Beamforming for Massive MIMO: A Survey," in IEEE Communications Magazine, vol. 55, no. 9, pp. 134-141, Sept. 2017.
- [7] X. Song, T. Kühne and G. Caire, "Fully-/Partially-Connected Hybrid Beamforming Architectures for mmWave MU-MIMO," in IEEE Transactions on Wireless Communications, vol. 19, no. 3, pp. 1754-1769, March 2020.
- [8] 3GPP, Technical Specification Group Radio Access Network; NR; Physical layer procedures for data (Release 15), 3GPP TS 38.214, v15.9.0, Dec. 2019.
- [9] R. Schmidt, "Multiple emitter location and signal parameter estimation," in IEEE Transactions on Antennas and Propagation, vol. 34, no. 3, pp. 276-280, March 1986
- [10] J. Wu, S. Kim and B. Shim, "Parametric Sparse Channel Estimation for RIS-Assisted Terahertz Systems," in IEEE Transactions on Communications, vol. 71, no. 9, pp. 5503-5518, Sept. 2023
- [11] C. R. Berger, Z. Wang, J. Huang and S. Zhou, "Application of compressive sensing to sparse channel estimation," in IEEE Communications Magazine, vol. 48, no. 11, pp. 164-174, November 2010
- [12] J. Kim, Y. Ahn, S. Kim and B. Shim, "Deep Learning-Aided Parametric Sparse Channel Estimation for Terahertz Massive MIMO Systems," in IEEE Transactions on Cognitive Communications and Networking, vol. 10, no. 6, pp. 2136-2148, Dec. 2024
- [13] H. Ju, S. Jeong, S. Kim, B. Lee and B. Shim, "Transformer-Assisted Parametric CSI Feedback for mmWave Massive MIMO Systems," in IEEE Transactions on Wireless Communications, vol. 23, no. 12, pp. 18774-18787, Dec. 2024
- [14] C. A. Balanis, Antenna Theory: Analysis and Design, 4th ed., Hoboken, NJ, USA: Wiley, 2016.
- [15] 3GPP, Technical Specification Group Radio Access Network; Study on channel model for frequencies from 0.5 to 100 GHz (Release 16), 3GPP TR 38.901, v16.1.0, Dec. 2019.